Two mammalian glucosamine-6-phosphate deaminases: a structural and genetic study

Rodrigo Arreola[a,*], Brenda Valderrama[b], Maria L. Morante[a], Eduardo Horjales[a,*]

[a] *Departamento de Medicina Molecular y Bioprocesos, Instituto de Biotecnología, Universidad Nacional Autónoma de México, PO Box 510-3, Cuernavaca, Morelos 62250, Mexico*

[b] *Departamento de Bioingenieria, Instituto de Biotecnología, Universidad Nacional Autónoma de México, PO Box 510-3, Cuernavaca, Morelos 62250, Mexico*

Received 10 March 2003; revised 9 May 2003; accepted 20 June 2003

First published online 20 August 2003

Edited by Richard Cogdell

Abstract Glucosamine-6-phosphate deaminase (EC 3.5.99.6) is an allosteric enzyme that catalyzes the reversible conversion of D-glucosamine-6-phosphate into D-fructose-6-phosphate and ammonium. Here we describe the existence of two mammalian glucosamine-6-phosphate deaminase enzymes. We present the crystallographic structure of one of them, the long human glucosamine-6-phosphate deaminase, at 1.75 Å resolution. Crystals belong to the space group $P2_12_12_1$ and present a whole hexamer in the asymmetric unit. The active-site lid (residues 162–182) presented significant structural differences among monomers. Interestingly the region with the largest differences, when compared with the *Escherichia coli* homologue, was found to be close to the active site. These structural differences can be related to the kinetic and allosteric properties of both mammalian enzymes.

Key words: *K*-type allosteric system; EST; Isoenzyme; *GNPI*; GlcN6P-deaminase; Ammonia capture and detoxification

1. Introduction

Glucosamine-6-phosphate deaminase (GlcN6P-deaminase, EC 3.5.99.6), formerly known as glucosamine-6-phosphate isomerase (EC 5.3.1.10), catalyzes the reversible conversion of GlcN6P into D-fructose-6-phosphate (Fru6P) and ammonium. Although the enzyme was initially described in pig kidney [1], it has been currently characterized in a variety of organisms such as *Escherichia coli* [2], *Candida albicans* [3], *Musca domestica* [4], *Plasmodium falciparum* [5], *Canis familiaris* [6], *Bos taurus* [7] and *Homo sapiens* [8,9].

The best-studied GlcN6P-deaminase is that from *E. coli* and has been characterized from the structural, catalytic and mechanistic points of view [10–14]. The functional unit of this particular enzyme is a hexamer of identical 29 kDa subunits [2]. The *E. coli* GlcN6P-deaminase is a *K*-type allosteric enzyme, which is activated by substrate cooperativity and by the allosteric activator *N*-acetyl-glucosamine-6-phosphate (GlcNAc6P) [15]. Crystallographic structures of the 'T' and the 'R' conformers allowed us to describe the allosteric transition of the *E. coli* GlcN6P-deaminase [13,14] and to propose a catalytic mechanism [10].

The mammalian GlcN6P-deaminases from *C. familiaris* [6], *B. taurus* [7] and *H. sapiens* [9] have been purified and their catalytic parameters determined. Whereas all of them catalyze the same reaction using GlcN6P and present allosteric activation by GlcNAc6P, their catalytic and allosteric properties show significant differences, which might constitute a paradox if only one GlcN6P-deaminase exists for each species. The kinetics obtained for the enzyme from *C. familiaris* (isolated from kidney) is a *K*-type allosteric system such as its *E. coli* homologue [6]. In contrast, the kinetics found for the enzymes from *B. taurus* (isolated from kidney) and the recombinant *H. sapiens* enzyme expressed in *E. coli* are both *V*-type-like allosteric systems [7,9]. Whereas the enzymes from human and bovine sources show a molecular mass of 32.5 kDa [9], the canine enzyme presents a molecular mass of 30.4 kDa [6].

The physiological function of the GlcN6P-deaminase in mammals is poorly understood. When cells of the baby-hamster kidney line BHK-21 are exposed to high ammonium concentrations, GlcN6P-deaminase activity is induced [16]. Under these conditions, the GlcN6P synthesizing activity from Fru6P and ammonium is the sole responsible for ammonium assimilation with the concomitant accumulation of UDP-*N*-acetyl-glucosamine [17]. Interestingly, the GlcN6P-deaminase preparation obtained from cells of this line was composed of two different proteins of 29.9 and 32.4 kDa [16]. The amino acid sequence of the amino terminus of each one of these proteins was determined, yielding fragments with 70% identity [16] and suggesting the existence of at least two isoenzymes.

The genes encoding GlcN6P-deaminase from mouse [18], hamster [19] and human [20] sources have been cloned and sequenced. All of them encode a protein product of 289 residues with a predicted molecular mass of 33 kDa, similar in size to that isolated from *B. taurus* kidney and to one of the enzymes isolated from BHK-21 cells. In this paper we present the identification of a putative second GlcN6P-deaminase gene encoding a product of 276 residues in the mouse and human genomes. To offer further insight into the structural basis of the different regulatory and catalytic properties of these two isoenzymes, we report the crystallographic structure of the 289-residue-long human enzyme at 1.75 Å resolution (PDB ID 1NE7) and a computer model of the novel 276-residue-long human enzyme.

*Corresponding authors. Fax: (52)-777-317 23 88.
E-mail addresses: arreola@ibt.unam.mx (R. Arreola), horjales@ibt.unam.mx (E. Horjales).

0014-5793/03/$22.00 © 2003 Published by Elsevier B.V. on behalf of the Federation of European Biochemical Societies.
doi:10.1016/S0014-5793(03)00896-2

2. Materials and methods

2.1. Purification of the human recombinant GlcN6P-deaminase

Recombinant expression of the human GlcN6P-deaminase encoded by the constitutive GNPI gene cloned in pTZ19R was achieved using the *E. coli* IBPC590R strain [21]. Pre-cultures were prepared by inoculating a single colony of the recombinant strain in 200 ml of LB medium plus ampicillin and incubated for 4 h at 30°C. Six flasks with 1 l of LB medium plus ampicillin were inoculated with 50 ml of the pre-culture and incubated for 8 h at 30°C. The cells were concentrated by centrifugation at 5000 rpm. The pellet was washed three times with 150 mM, KCl and the extract was prepared by sonication in 20 mM EDTA, 150 mM KCl and 100 mM Tris–HCl pH 7.7 and cleared by centrifugation. The supernatant was precipitated with ammonium sulfate and the 40–55% fraction, containing the GlcN6P-deaminase activity, was collected and stored for further analysis. When necessary, the precipitate was dialyzed overnight against 50 mM Tris–HCl pH 8.2. The enzyme was purified as described elsewhere [7] and concentrated to 10 mg ml^{-1}.

2.2. Enzyme crystallization

Many crystals were obtained using vapor diffusion in sitting drops at 18°C. The crystal selected for diffraction was grown in a drop containing 10 mg ml^{-1} protein with a well solution of 1.68 M ammonium sulfate, 10 mM *N*-acetyl-glucosamine-6-phosphate and 0.1 mM 2-deoxy-2-amino-D-glucitol-6-phosphate at pH 7. Crystals grew as long rods in 3 months, reaching dimensions of up to 0.15×1.5 mm.

2.3. Data collection

A solution with the same components and concentrations of the reservoir plus 35% w/v of trehalose was used as cryoprotectant. After soaking during 24 h, crystals were flash-cooled using annealing techniques [22] and thus a 94.6% complete diffraction data set (Table 1) up to 1.75 Å resolution was obtained at the Stanford Synchrotron Radiation Laboratory, in the Station BL 9-1 with a wavelength of 0.78 Å.

2.4. Data integration, molecular replacement and structure refinement

Diffraction data were integrated using the DENZO program [23] and scaled using the SCALA program from the CCP4 package [24]. The structure was solved using the molecular replacement method with the whole hexamer of the *E. coli* GlcN6P-deaminase (PDB entry 1DEA) as poly-alanine template with 266 residues used as the starting model. The refinement procedure was carried out using the CNS program [25] and the program O was used for model building [26]. In the model building steps we used *2fo-fc* and *fo-fc* electron-density maps of the whole asymmetric unit to construct the hexameric particle. Trials to refine the structure using non-crystallographic symmetries did not yield results better than 24% in *R*-value, thus we proceeded to determine the hexamer as six individual monomers (Table 1). In the final steps, *2fo-fc* and *fo-fc* electron-density average maps were used as well as annealed omit maps with a spherical omitted region. The omitted region was on the active-site cavity to better build the transition-state analogue (competitive inhibitor).

2.5. Structural analyses

The structural analysis of the final model was performed using the program O and coupled programs (see command LSQ_IMPROVE in program O) [27]. The electron-density average maps were calculated using the AVE and IMP programs from the RAVE package [27].

2.6. Genomic searches for GlcN6P-deaminase coding genes

Searches were performed upon the National Centre for Biotechnology Information databases GenBank [28] and ESTs (Expressed Sequence Tags database) [29]. Additional searches were performed upon the mouse full-length cDNAs public database from the RIKEN Mouse Gene Encyclopaedia Project [30]. We used the tBLASTn program, which compares a protein query sequence against a nucleotide sequence database dynamically translated in all possible reading frames [31]. The initial search, using the GenBank database, was performed using the human GlcN6P-deaminase amino acid sequence deduced from the cDNA reported by Nomura and collaborators in the HUGE Protein Database (KIAA0060 number) [20]. The results of this search showed significant alignments with the previously reported 289-residue-long GlcN6P-deaminases from mouse, hamster and human. Moreover, a different mouse sequence, only 276 residues long, was found from two sources, adult male testis and 8-day-old embryo. This novel sequence was also found in the RIKEN Mouse Gene Encyclopaedia Project [30]. A search performed upon the human genome using the short mouse GlcN6P-deaminase sequence as query allowed the identification of two different deduced peptide sequences: (1) one located in chromosome 5 which corresponded to the previously reported long human GlcN6P-deaminase and (2) a second short sequence in chromosome 4. The complete sequence for the short copy was obtained through inspection of the DNA sequence in that chromosome fragment (gi|13628777). Exon–intron boundaries were identified using the GENSCAN program [32]. All alignments were performed manually using the SEQLAB program of the GCG [33].

2.7. Modelling of the short human GlcN6P-deaminase

The structural model of the short human GlcN6P-deaminase was built using the long human GlcN6P-deaminase crystallographic structure as template. The calculations for energy minimization and molecular dynamics were performed using the Insight II program from Molecular Simulations Inc [34] and its modules (Homology, Biopolymer and Discover). The simulation was made with the transition-state analogue molecule in the active-site cavity and 19 crystallographic water molecules plus a water coat of 5 Å. We calculated 12 000 minimization iterations and 20 000 dynamic iterations of 1 fs at 300 K. The structural analysis was made using the O program [26].

Table 1
Refinement statistics and diffraction data statistics

Refinement statistics		Diffraction data statistics	
Final *R*	0.193(0.223)[a]	Cell parameters	109.87 Å (90°), 110.89 Å (90°), 180.88 Å (90°)
R_{free}	0.217(0.245)[a] (10% of unique reflections)	Space group	$P2_12_12_1$
RMS deviation from ideal values		Resolution	1.75 Å
Bond lengths	0.005 Å	Unique reflections	209 143
Bond angles	1.4°	Completeness	94.3(96.8)[a]
Dihedral angles	23.1°	Multiplicity	3.8(3.6)[a]
Improper angles	0.85°	R_{sym}[b]	0.052(0.224)[a]
Estimated coordinate error		Range resolution	1.74–29.48 Å
ESD from Luzzati plot	0.19 Å	Asymmetric unit and biological unit	one hexamer
ESD from SIGMAA	0.13 Å	*I*/sigma	9.9(3.4)[a]
Water molecules	2194		

[a]Values in parentheses correspond to the highest resolution bin: 1.75–1.86. The R_{free} value was obtained using cross-validation throughout the method and the test set selection was random.
[b]$R_{sym} = \Sigma|I_n - \langle I_n \rangle| / \Sigma I_n$.

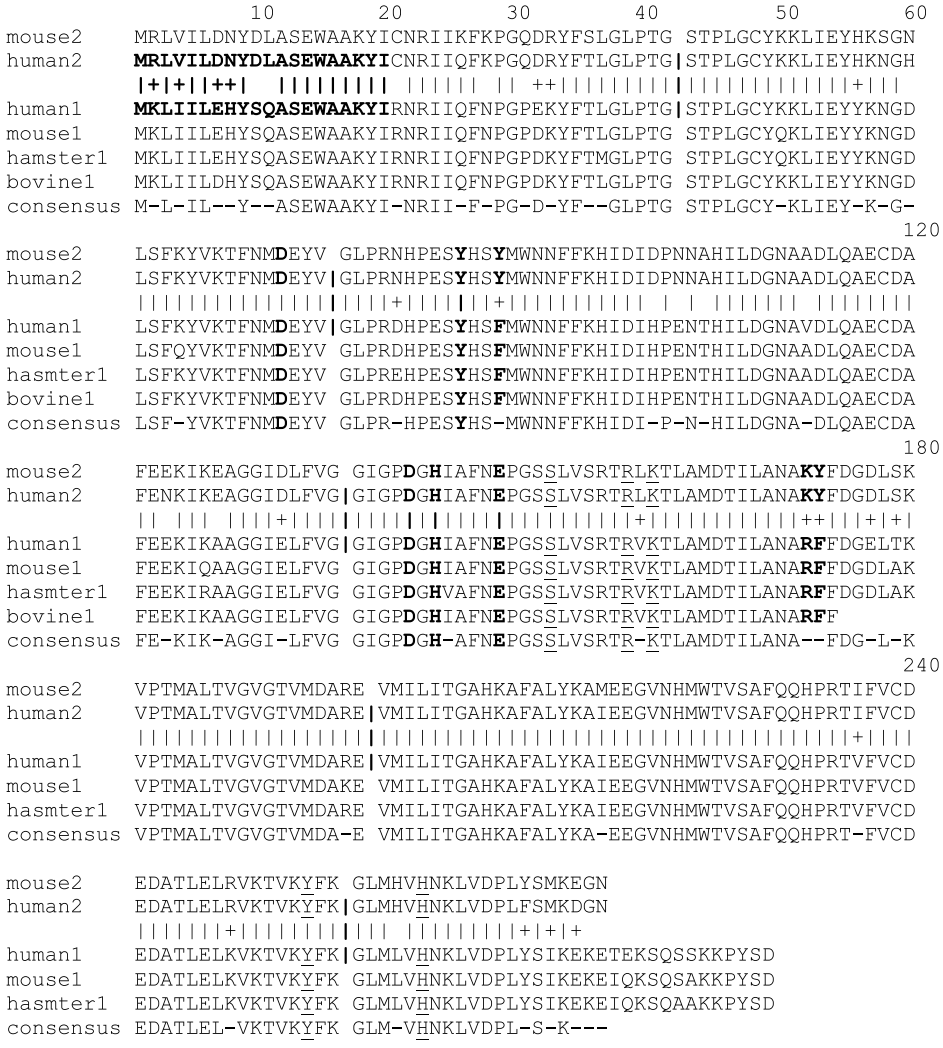

Fig. 1. Amino acid sequence alignment of mammalian GlcN6P-deaminases isoenzymes. The complete sequence of the orthologous *GNP1* gene products from human, mouse and hamster sources are shown, together with an incomplete product from bovine, with an overall identity ranging between 95.1 and 97.5%. Newly identified paralogous copies of *GNP1*, named *GNP2*, were found on the human and mouse genomes, with an identity of 96.8% between them. The first 20 residues of the amino terminus correspond to the sequence directly obtained from the two isoenzymes purified from the BHK-21 line cell [16]. The pipelines indicate the conserved exon–intron boundaries in human *GNP1* and *GNP2* transcripts. Conserved catalytic residues are highlighted in bold whereas allosteric-site residues are underlined.

3. Results

3.1. Sequence search and analyses

Two different sequences encoding putative GlcN6P-deaminases were detected in the human genome as described in Section 2 (Fig. 1). One of these sequences, which we named *GNP1*, is located in chromosome 5 (5q31) [35] and encodes a product of 289 residues with a predicted molecular mass of 32.6 kDa. This gene is actively transcribed in different tissues (Table 2). The deduced product of *GNP1* corresponds in size and sequence to the recombinant human GlcN6P-deaminase described elsewhere [7,9]. The second sequence, *GNP2*, is located in chromosome 4 (4p13) and encodes a product of 276 residues with a predicted molecular mass of 31.08 kDa. The functionality of *GNP2* was assessed by the identification of specific expression sequence tags from normal tissues and transformed cells (Table 2).

The products of *GNP1* and *GNP2* share 87% identity and 94.5% similarity throughout their sequences. Both genes are interrupted by five introns located at identical positions. Its is important to notice that the amino terminus of each one of these products matched with one of those obtained by direct sequencing of the enzymes purified from hamster cultured cells (Fig. 1) [16].

3.2. Crystallographic structure determination and refinement of the human GNP1

Crystals of the recombinant human GNP1 were obtained in complex with the allosteric activator GlcNAc6P, the competitive inhibitor 2-deoxy-2-amino-D-glucitol-6-phosphate, ammonia and inorganic sulfate (Table 1). The amount of unique reflections resulted enough to process the complete asymmetric unit and to refine individual atomic isotropic B factors. The three-dimensional structure was determined by molecular replacement using the structure of the hexamer of the *E. coli* GlcN6P-deaminase (PDB entry 1DEA) as initial model and was refined at 1.75 Å resolution. The final model has an $R = 0.20$ and an $R_{free} = 0.22$. The asymmetric unit contains six monomers (5×274 a.a.$+1 \times 281$ a.a.) with one allosteric activator, one trehalose molecule and one sulfate ion in alter-

nate conformation with a competitive inhibitor in each monomer. One additional sulfate ion appeared in the inter-hexameric crystal contacts. The C-terminal end presented an electron density visible only up to residue Glu274 in five of the six monomers in the asymmetric unit. Residues Lys275 to Gln289 were totally disordered in almost all the monomers, with the exception of monomer 'A' where a longer chain was visible up to residue 281 (Fig. 2). In this case, residues 278 to 281 showed crystalline contacts with a neighboring hexamer. No density was detected for residues 282 to 289 in monomer 'A'.

3.3. *High structural similarity of GNP1 with the* E. coli *enzyme, with the largest differences at the active-site region and in the C-terminus*

The asymmetric unit of GNP1 contained the biologically active particle, a hexamer with non-crystallographic 32 symmetry. A structural alignment by rigid-body superposition between the *E. coli* and the GNP1 hexamers showed an RMSD of 1.15 Å with 1560 α carbon atoms included in the superposition (260 α carbon atoms per monomer). The monomer fold was the same as in the *E. coli* enzyme [10].

3.4. *The C-terminus*

Although GNP1 and the *E. coli* enzymes share the same fold, GNP1 is longer in sequence and a rigid-body superposition between the two monomeric structures showed large differences in the main chain at the C-terminus starting at residue Leu258. In GNP1 a new structure was present with a short helix (residues 259 to 266) and an extended loop (residues 267 to 274) (Fig. 2). This extended loop builds an anchor of the helical structure (249–266), which supports the loop 240–249, responsible for the inter-monomeric interactions close to the two-fold axis of the hexameric particle. This inter-monomeric surface is rather flexible in the *E. coli* enzyme and is part of the core supporting the 13° rotation associated with the allosteric transition. The anchor in the C-terminus of the *E. coli* enzyme is much more flexible than the one found in GNP1 and this can be one of the structural properties generating the differences in allosteric behavior.

3.5. *The active site*

Many of the differences between GNP1 and the *E. coli* deaminases were located in the substrate-binding loops of the active site, in particular in the active-site lid (residues 162 to 182) and the phosphate-binding loop (residues 41 to 44). The α carbon atoms of these residues were more than 0.8 Å apart when both structures were superimposed (RMSD = 0.43 Å for 213 α carbons closer than 0.8 Å) (Fig. 3A).

A detailed analysis of the six active-site cavities in the different monomers of GNP1 showed a sulfate ion and a molecule of 2-deoxy-2-amino-D-glucitol-6-phosphate (the competitive inhibitor) in each active site, both molecules in alternate conformations. This molecules presented partial occupancy and shared similar coordinates in the phosphate-binding site. The rotamers of the catalytic residues were the same in the six monomers in the asymmetric unit.

The residues in the active site of the GNP1 and *E. coli* enzymes are fully conserved, with the remarkable exception of Ser43 (Gly in *E. coli*). This side chain is placed in good geometry to build a hydrogen bond with the phosphate moiety of the inhibitor (or the sulfate ion) in the human enzyme. Moreover, Ser43 is located in the phosphate-binding loop (residues 41–44), which is one of the few regions where significant differences appeared between geometries (Fig. 3). Residue Ser43 also appears in good geometry to bind Arg172, which is a substrate ligand, and therefore potentially able to compete with the substrate for this residue, leading to a conformational change of the active-site lid (residues 162–185).

Table 2
Expressed sequence tags for several *GNP1* and *GNP2* genes

Organism	Enzyme	Length (aa)	Entry type	Tissue	ID number
Human	1	1–289	Chromosomal	–	gi|13643897
Human	1	1–197	EST	Hypothalamus	gi|15494294
Human	1	1–213	EST	Testis	gi|15253870
Human	1	1–224	EST	Kidney	gi|13337909
Human	1	1–199	EST	Pancreatic islets	gi|180468
Human	2	1–276	Chromosomal	–	gi|13628777
Human	2	1–205	EST	Hypothalamus	gi|15490182
Human	2	1–140	EST	Testis	gi|13999823
Human	2	1–103	EST	Kidney	gi|5887273
Human	2	154–276	EST	Kidney	gi|13335729
Human	2	1–150	EST	Pancreatic islets	gi|15688350
Human	2	1–168	EST	Leiomyosarcoma line cells	gi|10346591
Human	2	1–166	EST	Adenocarcinoma line cells	gi|12613723
Mouse	1	1–289	cDNA	Testis	gi|5353760
Mouse	1	1–289	cDNA	Testis	gi|6754029
Mouse	2	1–276	cDNA	Testis	gi|12853906
Mouse	2	1–276	cDNA	8-day-old embryo	gi|12856903
Hamster	1	1–289	cDNA	Testis	gi|1177524
Bovine	1	1–42	Peptide	Kidney extraction	Lara-Lemus et al. [7]
Bovine	1	1–167	EST	Mammary tissues	gi|9607266
Bovine	1	1–155	EST	Mammary tissues	gi|9602899
Bovine	1	1–163	EST	Mammary tissues	gi|9596706
Bovine	1	57–174	EST	Mammary tissues	gi|6860672
Dog	1	158–289	cDNA	Testis	gi|18818168
Dog	2	208–276	cDNA	Heart	gi|23702059

The *GNP1* and *GNP2* genes encode three GlcN6P-deaminases enzymes in *H. sapiens*, *M. musculus* and *C. familiaris*. Both genes are actively expressed in several tissues and in four cases they are co-expressed (hypothalamus, testis, kidney and pancreatic islets).

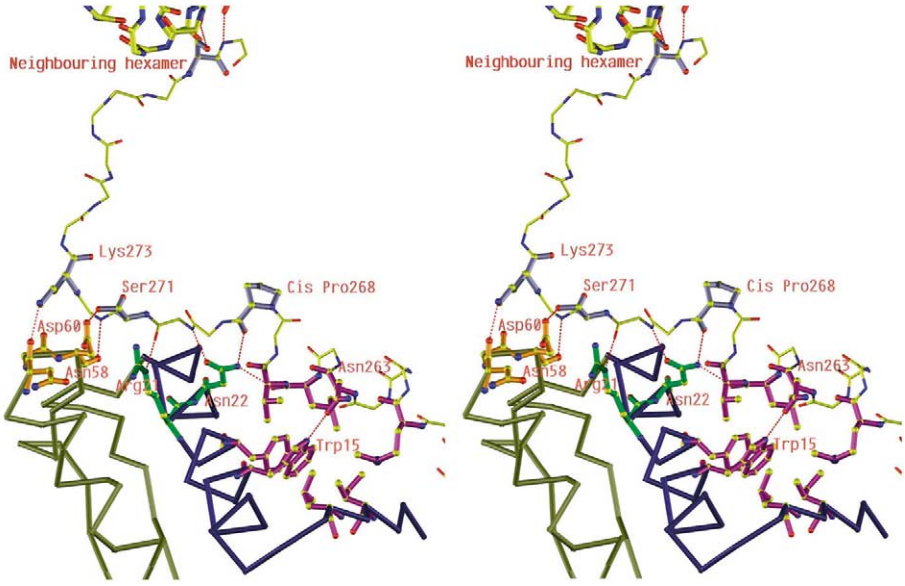

Fig. 2. Stereoscopic image of the human GNP1 C-terminus. The long C-terminus of the human GNP1 monomer A (from residue 259 onwards) interacts with the rest of the protein by hydrophobic interactions (residues Ile4, Leu6, Trp15, Tyr19, Met259, Leu265 and Val266 in purple) as well as a series of hydrogen bonds involving main chain and side chain residues (indicated by dashed red lines).

The lid presented conformational differences among the different monomers in the inhibitor-bound human enzyme (Fig. 3A), all different from the catalytic conformation of the lid found in the *E. coli* enzyme. We interpreted these differences as conformational disorder in the active site, which is a characteristic of GNP1. In the bacterial enzyme, a unique conformation of the active-site lid is observed when the inhibitor occupies this cavity, even when phosphate ions were used as precipitants at 2–4 M concentration [10]. All the mentioned conformational differences enlarged the GNP1 active-site cavity (as compared to the *E. coli* cavity) and changed the general coordination of the phosphate moiety in the substrate.

It is a very uncommon feature for the largest structural differences between orthologous enzymes to be located in the active site, in particular in the substrate-binding amino acids (Fig. 3A,B).

3.6. The allosteric site

The allosteric site in GNP1 is placed in a cleft between two monomers as in the *E. coli* enzyme [10]. Additionally, a new hydrogen bond between the activator O1 atom and the second monomer His262 NE2 atom was observed. This interaction, which is not present in the *E. coli* enzyme, might be related to the higher affinity observed in GNP1 for the allosteric activator [9,11]. His262 is part of the longer C-terminus GNP1 and is not present in the *E. coli* enzyme.

3.7. Computer model of the short human GlcN6P-deaminase

The products of *GNP1* and *GNP2* share an identity of 87% distributed evenly throughout the length of the alignment without gaps (Fig. 1). As expected, many of the differences were located at the surface of the protein. Nevertheless, some of these mutations appeared in positions close to the active site. These are Phe88Tyr, Phe173Tyr, and Arg172Lys (first the amino acid in GNP1 and afterwards the one in GNP2). The Phe to Tyr substitutions added hydroxyl groups to the side chains, generating close contacts (2.3 Å distance) with the phosphate-binding loop (residues 41–44). Additionally, new hydrogen bonds were built along the main chain of the loop without changing the hydrophobic interactions at side chains 88 and 173 present in the crystallographic structure of the long enzyme. Furthermore, both minimization and molecular dynamics procedures (see Section 2) relocate the phosphate-binding loop. The relocation approached the loop to the active-site cavity without changing the hydrophobic interactions around the aromatic rings of residues 88 and 173 (Fig. 4). This rearrangement might be sufficient for the stabilization of the active-site lid and the optimal binding conformation of the inhibitor.

4. Discussion

Here we present the identification of two GlcN6P-deaminase genes (*GNP1* and *GNP2*) in the completely sequenced genomes of human and mouse (Fig. 1). Kinetic and structural studies show that both enzymes share the same fold, both are hexameric particles in solution, present the same catalytic activity with the same substrates, and share the same allosteric activator [6,7,9]. Moreover, these genes are often expressed in the same tissues. However, their lengths are different (276 and 289) as well as some amino acids in the proximity of the active-site cavity. We found that 15 residues in the C-terminal region of GNP1 are completely disordered in the crystallographic structure. The amino acid sequence of this C-terminal segment is very uncommon, as more than 50% of the residues are charged. Our search for footprints within this sequence did not produce any positive result. We cannot assign any specific function for this segment.

The three-dimensional structure of GNP1 shows different conformations for the active-site lid in all the six independent monomers in the crystal. Interestingly, none of them corresponded to the conformation observed in the *E. coli* enzyme. Moreover, in all monomers, the phosphate-binding loop is displaced 1.0 Å from the position known to generate the cat-

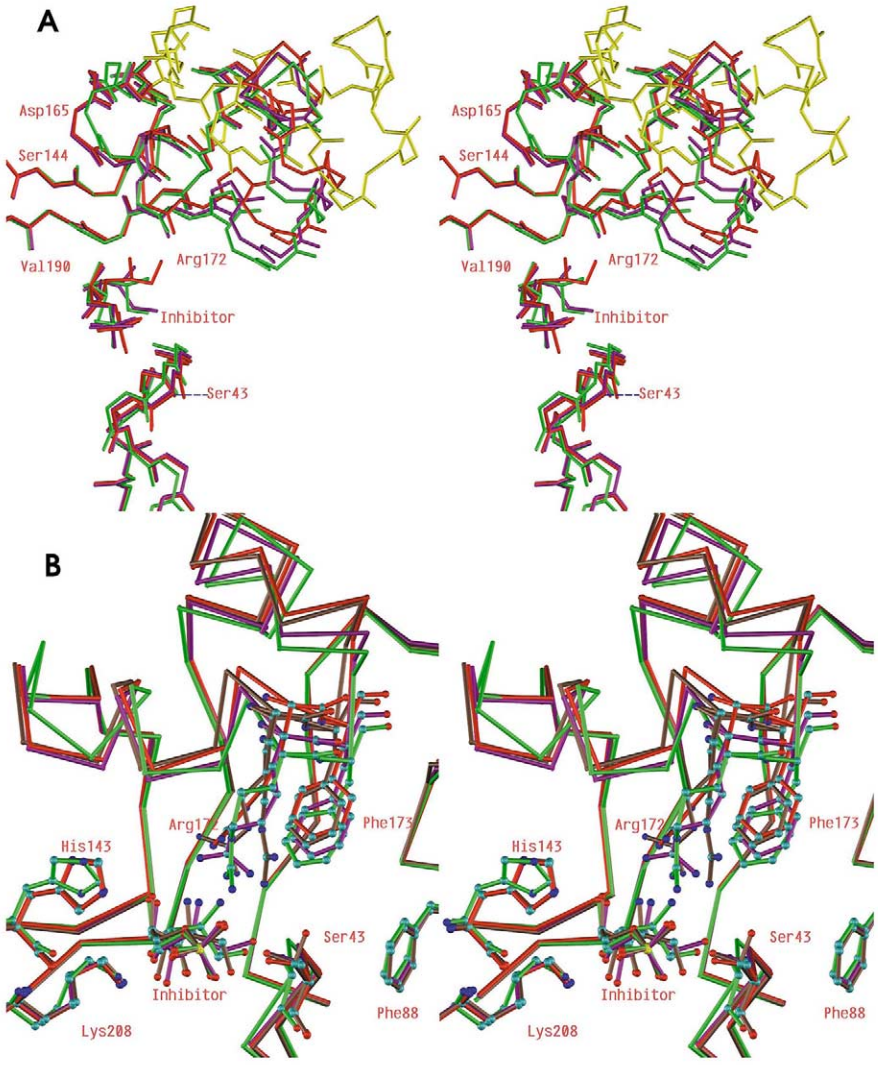

Fig. 3. Rigid-body superposition of the six monomers of human GNP1. The superposition leads to root mean-square deviations between 0.303 and 0.196 Å. The monomers B and F (chains in red and purple) presented the largest differences in the main chain of the active-site lid (residues 162–182). A: Conformations of the active-site loops in human and *E. coli* enzymes. The main chains of monomers A, C, D and E are not shown for simplicity. The active-site lid of monomer F presents an additional hydrogen bond between the Glu177 side chain and the main chain oxygen of Arg79 of a neighboring hexamer. The structure of the *E. coli* GlcN6P-deaminase in complex with the competitive inhibitor molecule is shown in green whereas the structure of the same enzyme free of active-site ligands is shown in yellow. Another significant difference between the human GNP1 and the *E. coli* enzyme is at the phosphate-binding loop at residue Ser43 where there is a distance of around 1 Å between corresponding Cα carbons. B: Conformational disorder at the active-site lid found in the human GlcN6P-deaminase-inhibitor complex. GlcN6P-deaminase chains shown are: A (chain in brown), B (chain in red) and F (chain in purple). The *E. coli* enzyme is represented in green. The side chains of Arg172 and Phe173 show conformational disorder in the active-site lid of the human enzyme. The monomer A has alternate conformations in Ser43 and Arg172. The alternative conformations of Ser43 show different interactions, one bound to the phosphate of the inhibitor (or sulfate ion) as well as to Arg 172 and the other bound only to Arg 172. This geometry is not observed in the *E. coli* enzyme.

alytic conformation in the *E. coli* enzyme. The phosphate moiety of the substrate is thus in a different position and the C1, O1, C2 and N2 atoms, which participate in the isomerization reaction, did not present electron density in most of the monomers. The catalytic reaction region is usually the most conserved portion of all enzymes. In contrast, the computer model of the human GNP2 presented the phosphate-binding loop in a conformation similar to that of the *E. coli* enzyme.

Two different allosteric systems (*V*- and *K*-type systems) have been reported in the literature for GlcN6P-deaminases isolated from bovine and canine kidneys. GNP1 can be identified with a *V*-type allosteric system, which is found in bovine and recombinant human enzymes [7,9]. We suggest that the product of the human and mouse *GNP2* genes might be identified with the *K*-type allosteric system isolated from canine kidney [6] given their similarity of molecular weights and differences observed in its kinetic behavior with that of the GNP1 product [7,9]. GNP2 seems to be significantly similar to the *E. coli* GlcN6P-deaminase in its kinetic behavior and in the active-site structure, and therefore we suggest that it can be a catabolic enzyme, optimized for reaction rate acceleration. In contrast, GNP1 is related to an unusually high affinity for ammonia (the *B. taurus* enzyme presents a K_m for ammo-

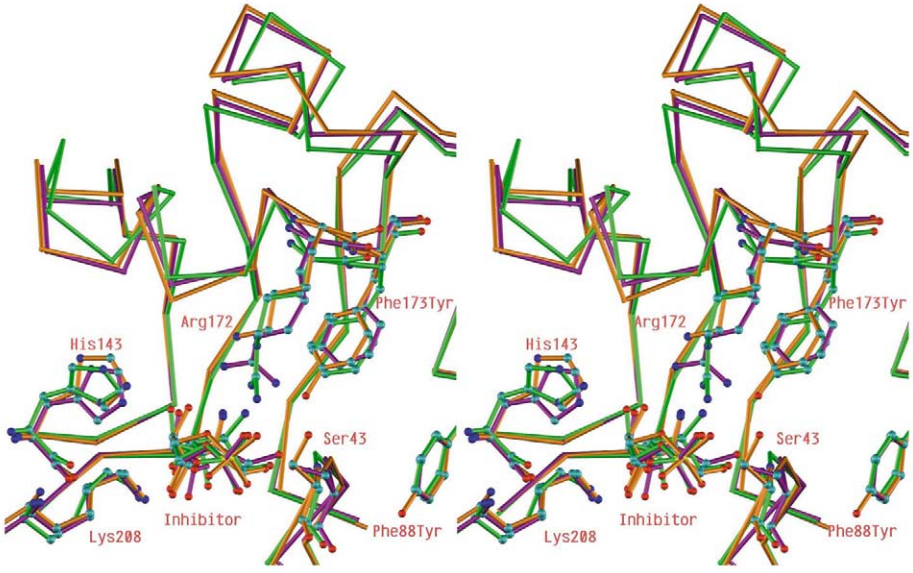

Fig. 4. Computer model of human GlcN6P-deaminase (GNP2). The crystallographic structure of GlcN6P-deaminase from *E. coli* is shown in green, aligned with the crystallographic structure of human GlcN6P-deaminase (monomer F, in purple). The F monomer presents the active-site lid in a conformation that builds the smallest active-site cavity. The orange chain is the minimization of the computer model of the *GNP2* gene product. This enzyme has two mutations in the active-site lid (residues 162–182): Arg172 is changed to Lys and Phe173 changed to Tyr. A third mutation neighboring the phosphate-binding loop (residues 40–45), is Phe88, which is also changed to Tyr. The changes in residues 88 and 173 add two OH groups, generating close contacts with the phosphate-binding loop. In these conditions, the energy minimization displaced this loop to a position similar to that observed in *E. coli* GlcN6P-deaminase.

nia of 3.7 mM) [7] in contrast to the *E. coli* enzyme with a K_m of 18 mM. [11]. Moreover, the structural differences observed around the active site of GNP1 when compared to the *E. coli* enzyme might be the result of a structural optimization towards a slightly different function as, for example, ammonia binding, since the transition-state analogue of the reaction binds in a disordered fashion.

Acknowledgements: We would like to thank Laura I. Álvarez-Añorve and Mario L. Calcagno for enzyme purification and Sonia Rojas for her technical assistance during enzyme crystallization. R.A. was recipient of a fellowship from Consejo Nacional de Ciencia y Tecnología. We are indebted to Nabuki Miyajima and J. Plumbridge for the *GNP1* gene. This work is based upon research conducted at Stanford Synchrotron Radiation Laboratory (SSRL) which is funded by Department of Energy (BES, BER) and the National Institute of Health (NCRR, NIGMS). We also want to thank Consejo Nacional de Ciencia y Tecnología for support (project 37120N).

References

[1] Leloir, L.F. and Cardini, C.E. (1956) Biochim. Biophys. Acta 20, 33–42.
[2] Calcagno, M., Campos, P.J., Mulliert, G. and Suastegui, J. (1984) Biochim. Biophys. Acta 787, 165–173.
[3] Das, M. and Datta, A. (1982) Biochem. Int. 5, 735–741.
[4] Benson, R.L. and Friedman, S. (1970) J. Biol. Chem. 245, 2219–2228.
[5] Weidans, J.A., Campbell, P., Moore, D., DeLucas, L.J., Rodén, L. and Vezza, A.C. (1995) Br. J. Haematol. 91, 578–586.
[6] Lara-Lemus, R., Libreros-Minotta, C.A., Altamirano, M.M. and Calcagno, M.L. (1992) Arch. Biochem. Biophys. 297, 213–220.
[7] Lara-Lemus, R. and Calcagno, M.L. (1998) Biophys. Acta 1388, 1–9.
[8] Weidanz, J.A., Campbell, P., DeLucas, L.J., Jin, J., Moore, D., Roden, L., Yu, H., Heilmann, E. and Vezza, A.C. (1995) Br. J. Haematol. 91, 72–79.
[9] Lara-Lemus, R. (1999) Ph.D. thesis, Universidad Nacional Autónoma de México, Facultad de Medicina, Ciudad de México.
[10] Oliva, G., Fontes, M.R., Garratt, R.C., Altamirano, M.M., Calcagno, M.L. and Horjales, E. (1995) Structure 3, 1323–1332.
[11] Montero-Moran, G.M., Lara-Gonzalez, S., Alvarez-Anorve, L.I., Plumbridge, J.A. and Calcagno, M.L. (2001) Biochemistry 40, 10187–10196.
[12] Bustos-Jaimes, I. and Calcagno, M.L. (2001) Arch. Biochem. Biophys. 394, 156–160.
[13] Rudiño-Piñera, E., Morales-Arrieta, S., Rojas-Trejo, S.P. and Horjales, E. (2002) Acta Crystallogr. D. Biol. Crystallogr. 58, 10–20.
[14] Horjales, E., Altamirano, M.M., Calcagno, M.L., Garratt, R.C. and Oliva, G. (1999) Structure 7, 527–537.
[15] Comb, D.G. and Roseman, S. (1958) J. Biol. Chem. 232, 807–827. See also Comb, D.G. and Roseman, S. (1962) Methods Enzymol. 5, 422–427.
[16] Çayli, A., Hirschmann, F., Wirth, M., Hauser, H. and Wagner, R. (1999) Biotechnol. Bioeng. 65, 192–200.
[17] Valley, U., Nimtz, M., Conradt, H.S. and Wagner, R. (1999) Biotechnol. Bioeng. 64, 401–417.
[18] Amireault, P. and Dube, F. (2000) Mol. Reprod. Dev. 56, 424–435. See also Montag, M., van der Ven, K., Dorbecker, C. and van der Ven, H. (1999) FEBS Lett. 458, 141–144.
[19] Wolosker, H., Kline, D., Bian, Y., Blackshaw, S., Cameron, A.M., Fralich, T.J., Schnaar, R.L. and Snyder, S.H. (1998) FASEB J. 12, 91–99. See also Parrington, J., Swann, K., Shevchenko, V.I., Sesay, A.K. and Lai, F.A. (1996) Nature 379, 364–368.
[20] Nomura, N., Nagase, T., Miyajima, N., Sazuka, T., Tanaka, A., Sato, S., Seki, N., Kawarabayasi, Y., Ishikawa, K. and Tabata, S. (1994) DNA Res. 1, 223–229. See also Suyama, M., Nagase, T. and Ohara, O. (1999) Nucleic Acids Res. 27, 338–339.
[21] Plumbrige, J.A., Cochet, O., Souza, J.M., Altamirano, M., Calcagno, M.L. and Badet, B. (1993) J. Bacteriol. 175, 4951–4956.
[22] Bunick, G., Harp, J., Timm, D. and Hanson, L. (1998) Rigaku J. 15, 6–12.
[23] Otwinowski, Z. (1993) in: Proceedings of the CCP4 Study Weekend: Data Collection and Processing (Sawyer, L., Issacs, N. and Baily, S., Eds.), pp. 56–62, SERC Daresbury Laboratory, Warrington. See also Otwinowski, Z. and Minor, W. (1996) in: Pro-

cessing of X-ray Diffraction Data Collected in Oscillation Mode (Carter, C. and Sweet, R.M., Eds.), pp. 307–325. Academic Press, Boston MA.
[24] Collaborative Computational Project, Number 4 (1994) Acta Crystallogr. D. Biol. Crystallogr. 50, 760–763.
[25] Brunger, A.T., Adams, P.D., Clore, G.M., Delano, W.L., Gros, P., Grosse-Kunstleve, R.W., Jiang, J.S., Kuszewski, J., Nilges, N., Pannu, N.S., Read, R.J., Rice, L.M., Simonson, T. and Warren, G.L. (1998) Acta Crystallogr. Sect. D. Biol. Crystallogr. 54, 905–921.
[26] Jones, T.A., Zou, J.Y., Cowan, S.W. and Kjeldgaard, M. (1991) Acta Crystallogr. A 47, 110–119.
[27] Kleywegt, G.J. and Jones, T.A. (2001) RAVE Package Version 010122/3.0, Uppsala University, Biomedical Centre, Uppsala.
[28] Benson, D.A., Karsch-Mizrachi, I., Lipman, D.J., Ostell, J., Rapp, B.A. and Wheeler, D.L. (2000) Nucleic Acids Res. 28, 15–18.
[29] Boguski, M.S. (1993) Nat. Genet. 4, 332–333.
[30] The RIKEN Genome Exploration Research Group Phase II Team and the FANTOM Consortium (2001) Nature 409, 685–690.
[31] Altschul, S.F., Madden, T.L., Schäffer, A.A., Zhang, J., Zhang, Z., Miller, W. and Lipman, D.J. (1997) Nucleic Acids Res. 25, 3389–3402.
[32] Burge, C. and Karlin, S. (1997) J. Mol. Biol. 268, 78–94.
[33] Wisconsin Package Version 10.2. (2001) Genetics Computer Group (GCG), Oxford Molecular Group, Inc., Madison, WI.
[34] Insight II, Version 98.0. (1998) Molecular Simulations Inc.
[35] Shevchenko, V., Hogben, M., Ekong, R., Parrington, J. and Lai, F.A. (1998) Gene 216, 31–38.